

# Fast Hankel Transform by Fast Sine and Cosine Transforms: The Mellin Connection

Luc Knockaert, *Member, IEEE*

**Abstract**—The Hankel transform of a function by means of a direct Mellin approach requires sampling on an exponential grid, which has the disadvantage of coarsely undersampling the tail of the function. A novel modified Hankel transform procedure that does not require exponential sampling is presented. The algorithm proceeds via a three-step Mellin approach to yield a decomposition of the Hankel transform into a sine, a cosine, and an inversion transform, which can be implemented by means of fast sine and cosine transforms.

**Index Terms**—Hankel transform, Mellin transform, sine and cosine transform.

## I. INTRODUCTION

THE NEED for numerical computation of the Hankel transform naturally arises in a variety of applications of technological interest, including optics [1], acoustics [2], electromagnetics [3], [4] and image processing [5]. Over the past 25 years, a number of algorithms for the numerical evaluation of the Hankel transform have been reported in the literature. For an overview of these algorithms and their numerical complexity, see [6]. Except for the obvious but inefficient numerical quadrature method, all these algorithms can be cast into three general classes. The first class consists of  $O(N \log_2 N)$  complexity Fourier-based algorithms via an exponential change of variables [7]–[10], which has the disadvantage of requiring sampling over an exponential grid, thereby leading to important errors in the Hankel transform of functions with an oscillating tail. The second class is based on the asymptotic expansion of the Bessel series in terms of sines and cosines [11], [12], leading to an  $O(N \log_2 N)$  complexity algorithm that is flawed, however, for small values of the output variable. The third class consists of the backprojection and projection-slice methods [12]–[18], which carry out the Hankel transform as a double integral by means of one of the standard integral representations of the Bessel functions. These projection methods generally require the efficient implementation of Tchebycheff and Abel transforms. The computational complexity of the projection-based algorithms unfortunately is  $O(N^2)$ , except in the case of Hansens's algorithm [15], where the overall complexity is  $O(N \log_2 N)$ . In this paper, we consider the Hankel transform in a direct Mellin setting, and we show that this leads to the Hankel transform methods by means of exponential sampling. Next, we show that a novel modified

Hankel transform approach with a three-step Mellin procedure leads to an algorithm consisting of a sine, a cosine, and an inversion transform, which can be carried out without requiring sampling over an exponential grid. Finally, the algorithm is implemented by means of the fast sine and cosine transform in  $O(N \log_2 N)$  complexity and applied to some pertinent numerical examples.

## II. DIRECT MELLIN APPROACH

Consider the Hankel transform

$$G(x) = \int_0^\infty J_\nu(xt)F(t)t dt \quad (1)$$

where  $J_\nu$  is the Bessel function of real order  $\nu$ . The Mellin transform [19], [20], which is defined as

$$\tilde{F}(s) = \int_0^\infty F(x)x^{s-1} dx \quad (2)$$

where  $\tilde{F}(s)$  is defined over its strip of convergence  $\sigma_1 < \Re s < \sigma_2$ , can be utilized to perform the Hankel transform (1). It is easy to prove [19] that the Hankel transform can be written in the Mellin domain as

$$\tilde{G}(s) = \tilde{J}_\nu(s)\tilde{F}(2-s) \quad (3)$$

where  $\tilde{J}_\nu(s)$  is given by the analytic formula

$$\begin{aligned} \tilde{J}_\nu(s) &= \int_0^\infty J_\nu(x)x^{s-1} dx \\ &= \frac{2^{s-1}\Gamma\left(\frac{\nu+s}{2}\right)}{\Gamma\left(\frac{\nu-s}{2}+1\right)} - \nu < \Re s < \nu+2 \end{aligned} \quad (4)$$

and where  $\Gamma$  is the Gamma function. Hence, the Hankel transform can be implemented using (3), requiring one direct and one inverse Mellin transform. Since the Mellin transform can be interpreted as a two-sided Laplace transform by the change of variables  $x = e^{-t}$ , i.e.,

$$\tilde{F}(s) = \int_0^\infty F(x)x^{s-1} dx = \int_{-\infty}^\infty e^{-st}F(e^{-t}) dt \quad (5)$$

it would seem that this could be easily implemented. If the strip of convergence of the Mellin or two-sided Laplace transform includes the imaginary axis  $s = i\omega$ , then the Mellin and inverse Mellin transforms can be replaced by a Fourier and an inverse Fourier transform, providing the basis for FFT-based algorithms

Manuscript received March 24, 1999; revised January 17, 2000. The associate editor coordinating the review of this paper and approving it for publication was Dr. Paulo J. S. G. Ferreira.

The author is with the Department of Information Technology, INTEC-IMEC, Gent, Belgium (e-mail: knockaert@intec.rug.ac.be).

Publisher Item Identifier S 1053-587X(00)04067-8.

[7]–[10]. However, the need to have  $F$  sampled on an exponential grid is a severe disadvantage since it amounts to a coarse undersampling of the tail away from the origin of the function  $F$  [6].

### III. MODIFIED MELLIN APPROACH

By means of the scaling transform pair

$$f(t) = 2t^{\nu/2} F(2\sqrt{t}) \quad (6)$$

$$g(x) = x^{-\nu/2} G(\sqrt{x}) \quad (7)$$

the Hankel transform (1) can be put in the more convenient modified form

$$g(x) = \int_0^\infty (xt)^{-\nu/2} J_\nu(2\sqrt{xt}) f(t) dt. \quad (8)$$

Applying the Mellin transform to (8), we obtain

$$\tilde{g}(s) = \frac{\Gamma(s)}{\Gamma(1+\nu-s)} \tilde{f}(1-s). \quad (9)$$

To avoid the problem of sampling on an exponential grid inherent in the direct Mellin formulation, as explained in the previous section, we interpret (8) as the result of a three-step procedure

$$f_a(x) = \frac{2}{\pi} \int_0^\infty \cos(xt) f(t) dt \quad (10)$$

$$f_b(x) = \int_0^\infty K(xt) f_a(t) dt \quad (11)$$

$$g(x) = \int_0^\infty \sin(xt) f_b(t) dt \quad (12)$$

where  $K$  is a kernel function to be determined. In the Mellin domain this translates to

$$\tilde{f}_a(s) = \frac{2}{\pi} \Gamma(s) \cos\left(\frac{\pi}{2}s\right) \tilde{f}(1-s) \quad (13)$$

$$\tilde{f}_b(s) = \tilde{K}(s) \tilde{f}_a(1-s) \quad (14)$$

$$\tilde{g}(s) = \Gamma(s) \sin\left(\frac{\pi}{2}s\right) \tilde{f}_b(1-s). \quad (15)$$

Since  $\tilde{g}(s)$  is given by (9) and taking advantage of the identity

$$\Gamma(s)\Gamma(1-s) = \frac{\pi}{\sin \pi s} \quad (16)$$

we obtain

$$\tilde{K}(s) = \frac{\Gamma(s)}{\Gamma(\nu+s)}. \quad (17)$$

To find the inverse Mellin transform of  $\tilde{K}(s)$ , we only consider values  $\nu \geq 0$ . For  $\nu = 0$ , we have  $\tilde{K}(s) = 1$ , yielding  $K(t) = \delta(1-t)$ , and hence

$$f_b(x) = \int_0^\infty \delta(1-xt) f_a(t) dt = x^{-1} f_a(x^{-1}) = \mathcal{T}(f_a)(x). \quad (18)$$

The inversion operator  $\mathcal{T}(f)$  is an isometry (unitary transform) over  $L_2[0, \infty]$  since we have

$$\begin{aligned} & \int_0^\infty \mathcal{T}(f)(x) \cdot \mathcal{T}(g)(x) dx \\ &= \int_0^\infty x^{-1} f(x^{-1}) \cdot x^{-1} g(x^{-1}) dx \\ &= \int_0^\infty f(x) \cdot g(x) dx. \end{aligned} \quad (19)$$

It should be noted that this proves that the modified Hankel transform of order zero is a unitary transform over  $L_2[0, \infty]$  since it consists of a combination of cosine, sine, and inversion transforms. For  $\nu > 0$ , we have [19]

$$K(t) = \frac{1}{\Gamma(\nu)} (1-t)^{\nu-1} \Upsilon(1-t) \quad (20)$$

where  $\Upsilon$  is the Heaviside function. This leads to

$$f_b(x^{-1}) x^{\nu-1} = \frac{1}{\Gamma(\nu)} \int_0^x (x-t)^{\nu-1} f_a(t) dt. \quad (21)$$

The expression on the right-hand side of (21) is known as the fractional Riemann–Liouville integral [21], [22], which, when  $\nu = n$  is a natural number, can be written as the repeated integral

$$\begin{aligned} & \frac{1}{(n-1)!} \int_0^x (x-t)^{n-1} f_a(t) dt \\ &= \int_0^x dx_{n-1} \int_0^{x_{n-1}} dx_{n-2} \cdots \int_0^{x_1} f_a(x_0) dx_0 \\ &= \mathcal{I}_0^n(f_a) \end{aligned} \quad (22)$$

where  $\mathcal{I}_0$  stands for the integration operator

$$\mathcal{I}_0(f)(x) = \int_0^x f(t) dt. \quad (23)$$

When  $\nu = n$  is a natural number (including zero), (18) and (21) can be compactly written as

$$f_b(x) = \mathcal{T}(x^{-n} \mathcal{I}_0^n(f_a))(x). \quad (24)$$

Hence, the only tools necessary for the modified integer-order Hankel transform are a cosine transform, a sine transform, repeated integrations, and the inversion operator  $\mathcal{T}$ . However, for  $n > 0$ , the repeated integrations in the *middle* of the algorithm are awkward to deal with, and we would like to transfer these repeated integrations to a preprocessing phase, i.e., *before* the actual algorithm starts. This problem is addressed by changing the modified Hankel transform of order  $\nu$  into the modified Hankel transform of order zero by putting

$$\int_0^\infty (xt)^{-\nu/2} J_\nu(2\sqrt{xt}) f(t) dt = \int_0^\infty J_0(2\sqrt{xt}) f_\nu(t) dt \quad (25)$$

where  $f_\nu$  is a function to be determined. In the Mellin domain, this is equivalent to

$$\frac{\Gamma(s)}{\Gamma(1+\nu-s)} \tilde{f}(1-s) = \frac{\Gamma(s)}{\Gamma(1-s)} \tilde{f}_\nu(1-s) \quad (26)$$

or

$$\tilde{f}_\nu(s) = \frac{\Gamma(s)}{\Gamma(\nu+s)} \tilde{f}(s) = \tilde{K}(s) \tilde{f}(s). \quad (27)$$

Equation (27) bears close relationship with the Weyl fractional integral [19], leading to the explicit expression

$$f_\nu(x) = \frac{1}{\Gamma(\nu)} \int_x^\infty (t-x)^{\nu-1} t^{-\nu} f(t) dt \quad (28)$$

which is valid for  $\nu > 0$ . For  $\nu = n$  (a natural number), this can be simplified to

$$f_n(x) = \mathcal{I}_\infty^n(f(x)x^{-n}) \quad (29)$$

where  $\mathcal{I}_\infty$  stands for the integration operator

$$\mathcal{I}_\infty(f)(x) = \int_x^\infty f(t) dt. \quad (30)$$

From (25) and (29), we see that the modified Hankel transform of order  $n$  can be obtained by repeated integrations, followed by a modified Hankel transform of order zero.

#### IV. NUMERICAL IMPLEMENTATION

We restrict ourselves to the zeroth-order modified Hankel transform since we have shown in the previous section how higher order modified Hankel transforms can be reduced to the zeroth-order transform. To stress that no exponential sampling is needed, we start by sampling the objective function  $f(t)$  on a linear grid with step  $\Delta$ , yielding the sample set  $\{f(k\Delta)\}$ . We then reconstruct the function  $f(t)$  by linear interpolation as

$$f(t) = \sum_{k=0}^{r-1} f(k\Delta) \phi\left(\frac{t}{\Delta} - k\right) + \epsilon_T(t) + \epsilon_I(t) \quad (31)$$

where  $\phi(t)$  is the linear interpolatory kernel, which is also known as the hat function

$$\phi(t) = (1 - |t|)\Upsilon(1 - |t|) \quad (32)$$

and  $\epsilon_T(t)$ ,  $\epsilon_I(t)$  are, respectively, the truncation and interpolation errors

$$\epsilon_T(t) = \sum_{k=r}^{\infty} f(k\Delta) \phi\left(\frac{t}{\Delta} - k\right) \quad (33)$$

$$\epsilon_I(t) = f(t) - \sum_{k=0}^{\infty} f(k\Delta) \phi\left(\frac{t}{\Delta} - k\right). \quad (34)$$

The  $L_2$  norm of the truncation error satisfies

$$\|\epsilon_T\| = \sqrt{\int |\epsilon_T(t)|^2 dt} \leq \sqrt{2\Delta/3} \sum_{k=r}^{\infty} |f(k\Delta)| \quad (35)$$

since  $\|\phi\| = \sqrt{2/3}$ . Hence, the truncation error is small, provided  $|f(t)|$  has a fast decreasing tail for  $t \geq r\Delta$ . Note that in general,  $\|\epsilon_T\| \rightarrow 0$  for  $r \rightarrow \infty$ , provided  $\sup_t |f(t)|t^\eta < \infty$  for some  $\eta > 1$ . The interpolation error mainly depends on the

smoothness of the function  $f(t)$  and the quasi-interpolant character of the kernel  $\phi(t)$ . It has been proved in [23] that the  $L_2$  norm of the interpolation error satisfies

$$\|\epsilon_I\| \leq C\Delta^q \|f^{(q)}\| \quad (36)$$

provided  $f(t)$  has its  $q$ th derivative in  $L_2[0, \infty]$  and provided the interpolation kernel is a quasi-interpolant of order  $q$ , i.e.,

$$\sum_{k \in \mathbb{Z}} k^m \phi(x-k) = x^m \quad m = 0, \dots, q-1. \quad (37)$$

This is the case for the linear interpolatory kernel  $\phi(t)$  for which  $q = 2$ . Note that in general,  $\|\epsilon_I\| \rightarrow 0$  for  $\Delta \rightarrow 0$ . Since the zeroth-order modified Hankel transform is unitary, the truncation and interpolation errors propagate through the transform process with their  $L_2$  norms unchanged, and hence, we can as well omit the error terms in (31) and consider the modified Hankel transform of

$$\bar{f}(t) = \sum_{k=0}^{r-1} f(k\Delta) \phi\left(\frac{t}{\Delta} - k\right) \quad (38)$$

while acknowledging the existence of the error norms  $\|\epsilon_I\|$  and  $\|\epsilon_T\|$ . After the cosine transform of (38), we obtain

$$f_a(x) = \frac{2}{\pi} U_\Delta(x) \sum_{k=0+}^{r-1} f(k\Delta) \cos(xk\Delta) \quad (39)$$

where  $\sum_{k=0+}^{r-1} a_k = (1/2)a_0 + a_1 + \dots + a_{r-1}$ , and  $U_\Delta(x)$  is the Fourier transform

$$U_\Delta(x) = \int_{-\infty}^{\infty} e^{-ixt} \phi(t/\Delta) dt = \Delta \left( \frac{\sin \Delta x/2}{\Delta x/2} \right)^2. \quad (40)$$

Note that equations (39) and (40) imply

$$f_b(0) = \lim_{x \rightarrow 0} x^{-1} f_a(x^{-1}) = \lim_{x \rightarrow \infty} x f_a(x) = 0. \quad (41)$$

Sampling at multiples of the new step

$$\Delta_c = \frac{\pi}{N\Delta} \quad (42)$$

where  $N \geq r$  is a power of two, leads to

$$f_a(l\Delta_c) = \frac{2}{\pi} U_\Delta(l\Delta_c) \sum_{k=0+}^{r-1} f(k\Delta) \cos(kl\pi/N) \quad (43)$$

$$l = 0, 1, \dots, M-1$$

where  $M = Nm$ , and  $m$ , which is the oversampling rate, is chosen to be a power of two. Oversampling is necessary to adequately represent the tail of the function  $f_a$  since it is easy to prove that

$$\max_{l \geq M} |f_a(l\Delta_c)| \leq \frac{\Delta}{m^2} \left( \frac{2}{\pi} \right)^3 \sum_{k=0+}^{r-1} |f(k\Delta)|. \quad (44)$$

Formula (43) can be efficiently implemented with the fast cosine transform [24] with possible zero padding ( $r < N$ ). Note that

we only need two fast cosine transforms of order  $N$  since the modulo  $N$  decomposition of the index  $l = N\alpha + \beta$  implies that

$$\sum_{k=0+}^{r-1} f(k\Delta) \cos(kl\pi/N) = \sum_{k=0+}^{r-1} (-1)^{k\alpha} f(k\Delta) \cos(k\beta\pi/N). \quad (45)$$

Next, we interpolate  $f_a(x)$  at the chosen data points, yielding

$$f_a(x) = \sum_{l=0}^{M-1} f_a(l\Delta_c) \phi\left(\frac{x}{\Delta_c} - l\right) + \epsilon_T^a(x) + \epsilon_I^a(x) \quad (46)$$

where the same error analysis as before is applicable. Omitting the error terms  $\epsilon_T^a$  and  $\epsilon_I^a$ , we may write

$$\bar{f}_a(x) = \sum_{l=0}^{M-1} f_a(l\Delta_c) \phi\left(\frac{x}{\Delta_c} - l\right). \quad (47)$$

To find an adequate representation of the function  $f_b(x) = x^{-1}\bar{f}_a(x^{-1})$ , we split (47) as

$$\begin{aligned} \bar{f}_a(x) &= \sum_{l=0}^p f_a(l\Delta_c) \phi\left(\frac{x}{\Delta_c} - l\right) \\ &\quad + \sum_{l=p+1}^{M-1} f_a(l\Delta_c) \phi\left(\frac{x}{\Delta_c} - l\right) \\ &= f_{a1}(x) + f_{a2}(x) \end{aligned} \quad (48)$$

where  $p \geq 1$ . In fact, as will be seen from the numerical examples, taking the lowest possible value plus one, i.e.,  $p = 2$ , seems to be a judicious choice. The reason for the splitting (48) is that the functions  $\phi(x^{-1})$  and  $\phi(x^{-1} - 1)$  do not have compact support, and in general, the functions  $\phi(x^{-1} - l)$  with  $l$  small will represent functions with a support that is too large to fit in a subsequent interpolatory scheme. Therefore, the sine transform (12) of  $f_{b1}(x) = x^{-1}f_{a1}(x^{-1})$  is calculated analytically, yielding

$$\begin{aligned} g_1(x) &= \sum_{l=0}^p f_a(l\Delta_c) \int_0^\infty \sin(xt) t^{-1} \phi\left(\frac{t^{-1}}{\Delta_c} - l\right) dt \\ &= \sum_{l=0}^p f_a(l\Delta_c) \Theta_l(x/\Delta_c) \end{aligned} \quad (49)$$

where the functions  $\Theta_k$ , bearing close relationship with the sine and cosine integrals, are derived in the Appendix.

To sample the function  $f_{b2}(x) = x^{-1}f_{a2}(x^{-1})$ , we must first choose the sampling step. It is clear from (41) that we must take  $f_{b2}(0) = 0$  as a first sample. If we take as sampling step

$$\Omega = \frac{1}{(M-1)\Delta_c} \quad (50)$$

the second sample of  $f_{b2}$  corresponds with the  $M$ th sample of  $f_{a2}$ . The other samples are obtained by linear interpolation. Summarizing, we have

$$f_{b2}(0) = 0 \quad (51)$$

$$f_{b2}(k\Omega) = 0 \quad k \geq \frac{M-1}{p} \quad (52)$$

$$f_{b2}(\Omega) = \frac{1}{\Omega} f_a((M-1)\Delta_c) \quad (53)$$

else

$$\begin{aligned} f_{b2}(k\Omega) &= \frac{1}{k\Omega} \left\{ f_a(l_k\Delta_c) + \left( \frac{M-1}{k} - l_k \right) \right. \\ &\quad \left. \cdot (f_a((l_k+1)\Delta_c) - f_a(l_k\Delta_c)) \right\} \end{aligned} \quad (54)$$

where

$$l_k = \left\lfloor \frac{M-1}{k} \right\rfloor \quad (55)$$

and  $\lfloor \cdot \rfloor$  is the floor function. This leads to the interpolation formula

$$f_{b2}(x) = \sum_{l=0}^{M-1} f_{b2}(l\Omega) \phi\left(\frac{x}{\Omega} - l\right) + \epsilon_T^b(x) + \epsilon_I^b(x) \quad (56)$$

where the same error analysis as before is applicable. Omitting the error terms  $\epsilon_T^b$  and  $\epsilon_I^b$ , we may write

$$\bar{f}_{b2}(x) = \sum_{l=0}^{M-1} f_{b2}(l\Omega) \phi\left(\frac{x}{\Omega} - l\right) \quad (57)$$

yielding the sine transform

$$g_2(x) = U_\Omega(x) \sum_{k=0}^{M-1} f_{b2}(k\Omega) \sin(xk\Omega) \quad (58)$$

and its sampled version

$$\begin{aligned} g_2(l\Delta_s) &= U_\Omega(l\Delta_s) \sum_{k=0}^{M-1} f_{b2}(k\Omega) \sin(kl\pi/M) \\ &\quad l = 0, 1, \dots, M-1 \end{aligned} \quad (59)$$

where

$$\Delta_s = \frac{\pi}{M\Omega}. \quad (60)$$

Formula (59) can be efficiently implemented with the fast sine transform [24]. Finally,  $g(x)$  can be written as

$$\begin{aligned} g(x) &= \sum_{l=0}^{M-1} [g_1(l\Delta_s) + g_2(l\Delta_s)] \phi\left(\frac{x}{\Delta_s} - l\right) \\ &\quad + \epsilon_T^g(x) + \epsilon_I^g(x) \end{aligned} \quad (61)$$

where the same error analysis as before is applicable. An important point is the choice of the sampling steps  $\Delta$ ,  $\Delta_c$ ,  $\Omega$  and  $\Delta_s$ . If we require the input step  $\Delta$  to be approximately equal to the output step  $\Delta_s$ , it is easy to show that  $\sqrt{N} \approx \pi/\Delta$ , and hence, a reasonable choice for  $N$  is

$$N = 4^{\lceil \log_2(\pi/\Delta) \rceil}. \quad (62)$$

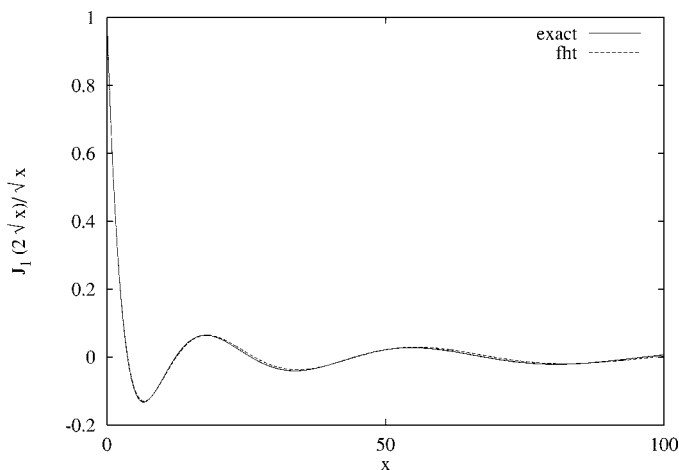
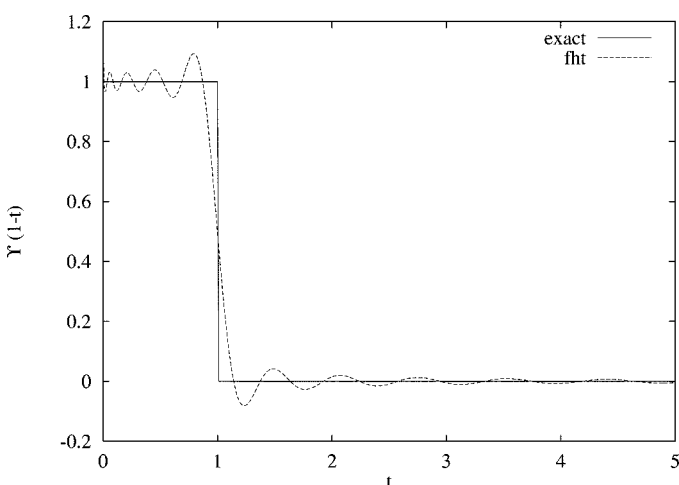
When  $N$  is chosen this way, all the sampling steps are of the same order of magnitude since it is then clear that

$$\Delta_s \approx \Delta \quad \Delta_c \approx \Delta/\pi \quad \Omega \approx \Delta/m\pi. \quad (63)$$

The operation count is given by

$$\text{NOP} = 2N \log_2 N + M \log_2 M + (p+1+\gamma)M \quad (64)$$

where the constant  $\gamma$  summarizes the overhead due to the multiplications with the kernel  $U_\Delta$  and the linear interpolations at the core of the algorithm.


 Fig. 1. Modified Hankel transform pair  $\Upsilon(1-t) \mapsto J_1(2\sqrt{x})/\sqrt{x}$ .

 Fig. 2. Modified Hankel transform pair  $J_1(2\sqrt{x})/\sqrt{x} \mapsto \Upsilon(1-t)$ .

## V. NUMERICAL RESULTS

- As a first example, we consider the modified Hankel transform pair

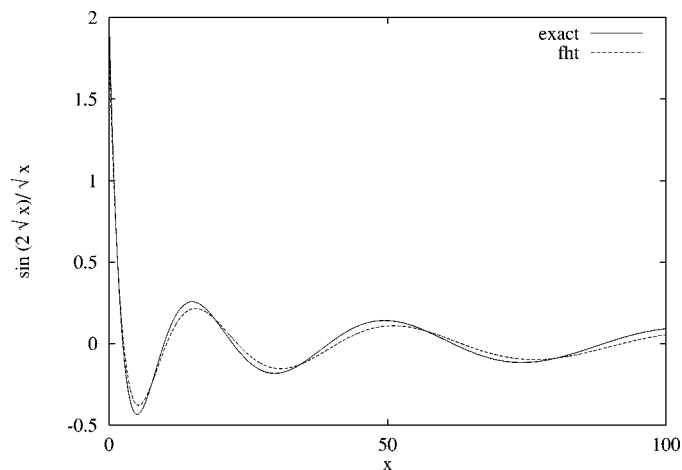
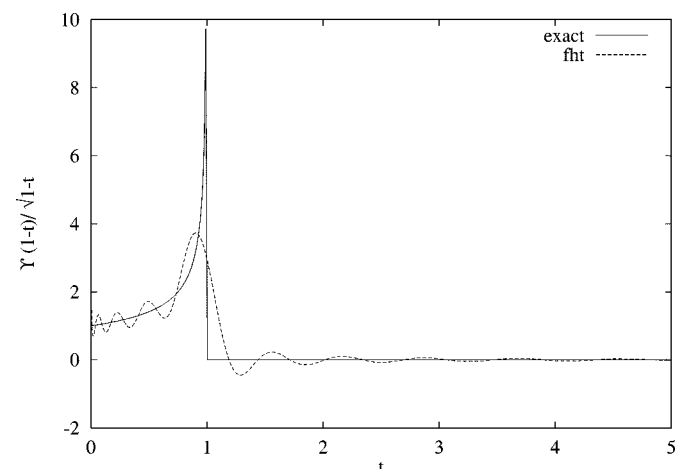
$$f(t) = \Upsilon(1-t) \quad g(x) = J_1(2\sqrt{x})/\sqrt{x}. \quad (65)$$

The direct transform  $f \rightarrow g$  is performed with  $r = 64$  samples, a sampling range  $r\Delta = 2.0$ , an oversampling rate  $m = 4$ , and a parameter  $p = 2$ . The resulting curve is shown in Fig. 1. The inverse transform  $g \rightarrow f$  is more difficult to implement since to have a finite sampling range, we need to cut off the tail of  $g$ , causing truncation errors, whereas Gibbs-type ringing errors occur due to the fact that the outcome of the transform  $f$  is not a continuous function. The resulting curve, with  $r = 4096$ ,  $r\Delta = 200.0$ ,  $m = 4$ , and  $p = 2$ , is shown in Fig. 2.

- As a second example, we consider the modified Hankel transform pair

$$f(t) = \Upsilon(1-t)/\sqrt{1-t} \quad g(x) = \sin(2\sqrt{x})/\sqrt{x}. \quad (66)$$

The direct transform  $f \rightarrow g$  and inverse transform  $g \rightarrow f$  are executed with respective parameters  $r = 128$ ,  $r\Delta = 2.0$ ,  $m = 4$ ,  $p = 2$  and  $r = 4096$ ,  $r\Delta = 197.0$ ,  $m = 4$ ,  $p = 2$ . The results are shown in Figs. 3 and 4. It is


 Fig. 3. Modified Hankel transform pair  $\Upsilon(1-t)/\sqrt{1-t} \mapsto \sin(2\sqrt{x})/\sqrt{x}$ .

 Fig. 4. Modified Hankel transform pair  $\sin(2\sqrt{x})/\sqrt{x} \mapsto \Upsilon(1-t)/\sqrt{1-t}$ .

seen that the remarks from the first example regarding the inverse transform apply to this example in an even enhanced fashion, due to the fact that  $f$  exhibits a singularity at  $t = 1$ . It should be noted that this example does not fit readily in the setting of the algorithm since we tacitly assumed  $f$  to be in  $C[0, \infty]$  (piece-wise linear = continuous) and  $L_2[0, \infty]$ , and in this example,  $f$  is neither.

- As a third example, we consider the modified Hankel transform pair

$$f(t) = 2e^{-2\sqrt{t}} \quad g(x) = (1+x)^{-3/2}. \quad (67)$$

Both the direct and inverse transforms are performed with the same parameter set  $r = 128$ ,  $r\Delta = 10.0$ ,  $m = 2$ ,  $p = 2$ . The results are shown in Figs. 5 and 6.

- Finally, we consider the modified Hankel transform pair

$$f(t) = L_8(2t)e^{-t} \quad g(x) = L_8(2x)e^{-x} \quad (68)$$

where  $L_n$  stands for the Laguerre polynomial. Note that we have in general [25]

$$\int_0^\infty J_0(2\sqrt{xt}) L_n(2t)e^{-t} dt = (-1)^n L_n(2x)e^{-x} \quad (69)$$

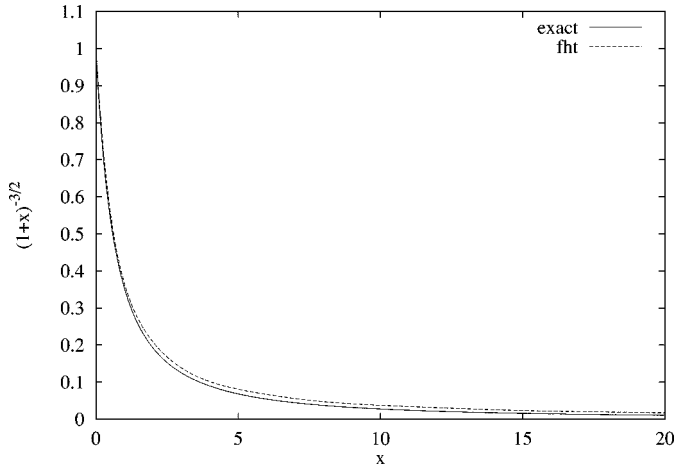


Fig. 5. Modified Hankel transform pair  $2e^{-2\sqrt{t}} \mapsto (1+x)^{-3/2}$ .

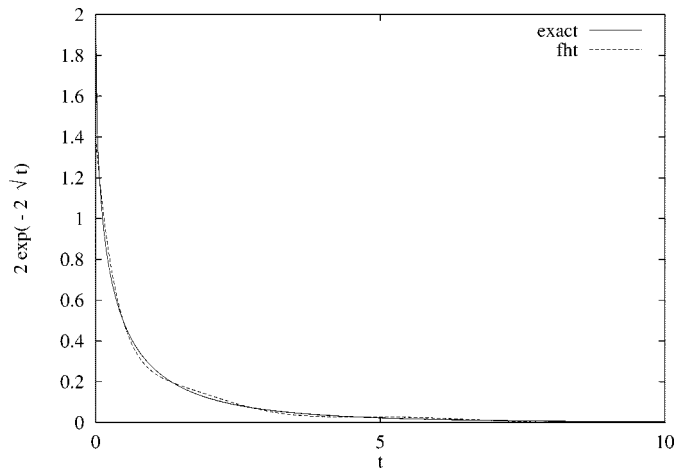


Fig. 6. Modified Hankel transform pair  $(1+x)^{-3/2} \mapsto 2e^{-2\sqrt{t}}$ .

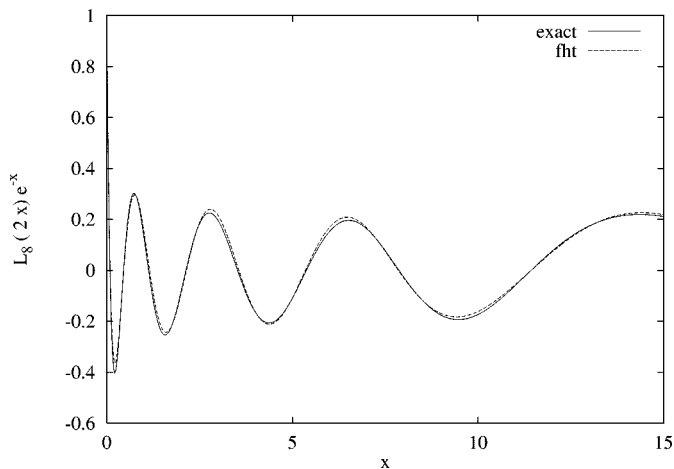


Fig. 7. Modified Hankel transform pair  $L_8(2t)e^{-t} \mapsto L_8(2x)e^{-x}$ .

and hence, the Laguerre functions (scaled by a factor two) are the eigenvectors of the modified Hankel transform with eigenvalues 1 and  $-1$ . The results for this last example, with parameter set  $r = 256$ ,  $r\Delta = 20.0$ ,  $m = 4$ ,  $p = 2$ , are shown in Fig. 7.

## VI. CONCLUSION

We have shown that a novel modified Hankel transform approach with a three-step Mellin procedure leads to an algorithm consisting of a sine, a cosine, and an inversion transform, which can be carried out without requiring sampling over an exponential grid. The algorithm is implemented by means of the fast sine and cosine transform, together with judiciously chosen interpolation schemes, yielding an  $O(N \log_2 N)$  complexity algorithm.

## APPENDIX

In order to evaluate (49), we need to find an expression for

$$\Theta_k(x) = \int_0^\infty \sin(xt)t^{-1}\phi(t^{-1}-k)dt. \quad (\text{A1})$$

After some algebra, we obtain

$$\Theta_0(x) = \frac{\pi}{2} - S(x) \quad (\text{A2})$$

where the function  $S(x)$  is given by

$$S(x) = \text{Si}(x) + \sin x - x\text{Ci}(x) \quad (\text{A3})$$

and where  $\text{Si}(x)$  and  $\text{Ci}(x)$  are the sine and cosine integral functions [26] defined as

$$\text{Si}(x) = \int_0^x \sin(u)u^{-1}du \quad (\text{A4})$$

$$\text{Ci}(x) = -\int_x^\infty \cos(u)u^{-1}du. \quad (\text{A5})$$

Programs for the computation of these functions are available, e.g., in the Numerical Recipes [24] packages. In the same vein, we have

$$\Theta_1(x) = 2S(x) - 2S(x/2) \quad (\text{A6})$$

and for  $k > 1$ , we have the expression

$$\Theta_k(x) = 2kS(x/k) - (k-1)S(x/(k-1)) - (k+1) \cdot S(x/(k+1)). \quad (\text{A7})$$

## REFERENCES

- [1] A. Papoulis, *Systems and Transforms with Applications in Optics*. New York: McGraw-Hill, 1968.
- [2] L. M. Brekhovskikh, *Waves in Layered Media*. New York: Academic, 1960.
- [3] R. Hsieh and J. Kuo, "Fast full-wave analysis of planar microstrip circuit elements in stratified media," *IEEE Trans. Microw. Theory Tech.*, vol. 46, pp. 1291–1297, Sept. 1998.
- [4] K. A. Michalski, "Extrapolation methods for Sommerfeld integral tails," *IEEE Trans. Antennas Propagat.*, vol. 46, pp. 1405–1418, Oct. 1998.
- [5] W. E. Higgins and D. C. Munson, "A Hankel transform approach to tomographic image reconstruction," *IEEE Trans. Med. Imag.*, vol. 7, pp. 59–72, 1988.
- [6] M. J. Cree and P. J. Bones, "Algorithms to numerically evaluate the Hankel transform," *Comput. Math. Appl.*, pp. 1–12, 1993.
- [7] A. E. Siegman, "Quasi fast Hankel transform," *Opt. Lett.*, vol. 1, no. 1, pp. 13–15, July 1977.
- [8] J. P. Talman, "Numerical Fourier and Bessel transforms in logarithmic variables," *J. Comput. Phys.*, vol. 29, pp. 35–48, 1978.
- [9] H. K. Johansen and K. Sorensen, "Fast Hankel transforms," *Geophys. Prospect.*, vol. 27, pp. 876–901, 1979.
- [10] A. Agnesi, G. C. Reali, G. Patrini, and A. Tomaselli, "Numerical evaluation of the Hankel transform: Remarks," *J. Opt. Soc. Amer.*, vol. 10, no. 9, pp. 1872–1874, Sept. 1993.

- [11] O. A. Sharafeddin, H. F. Bowen, D. J. Kouri, and D. K. Hoffman, "Numerical evaluation of spherical Bessel transforms via fast Fourier transforms," *J. Comput. Phys.*, vol. 100, pp. 294–296, 1992.
- [12] S. M. Candel, "Dual algorithms for fast calculation of the Fourier–Bessel transform," *IEEE Trans. Acoust., Speech, Signal Processing*, vol. ASSP-29, pp. 963–972, Oct. 1981.
- [13] A. V. Oppenheim, G. V. Frisk, and D. R. Martinez, "An algorithm for the numerical evaluation of the Hankel transform," *Proc. IEEE*, vol. 66, pp. 264–265, Feb. 1978.
- [14] —, "Computation of the Hankel transform using projections," *J. Acoust. Soc. Amer.*, vol. 68, no. 2, pp. 523–529, Aug. 1980.
- [15] E. W. Hansen, "Fast Hankel transform algorithm," *IEEE Trans. Acoust., Speech, Signal Processing*, vol. ASSP-33, pp. 666–671, June 1985.
- [16] W. E. Higgins and D. C. Munson, "An algorithm for computing general integer-order Hankel transforms," *IEEE Trans. Acoust., Speech, Signal Processing*, vol. ASSP-35, pp. 86–97, Jan. 1987.
- [17] Y. J. He, A. Cai, and J. A. Sun, "Real-valued Hankel transform approach to image reconstruction from projections," *Electron. Lett.*, vol. 29, no. 20, pp. 1750–1752, Sept. 1993.
- [18] V. P. Pauca, B. L. Ellerbroek, N. P. Pitsianis, R. J. Plemmons, and X. Sun, "Performance modeling of adaptive-optics imaging systems using fast Hankel transforms," *Proc. SPIE*, pp. 339–347, July 1998.
- [19] I. H. Sneddon, *The Use of Integral Transforms*. New York: McGraw-Hill, 1972.
- [20] R. Sasiela, *Electromagnetic Waves in Turbulence*. New York: Springer, 1994.
- [21] K. B. Oldham and J. Spanier, *The Fractional Calculus*. New York: Academic, 1974.
- [22] N. Engheta, "On the role of fractional calculus in electromagnetic theory," *IEEE Antennas Propagat. Mag.*, vol. 39, pp. 35–46, Aug. 1997.
- [23] M. Unser and I. Daubechies, "On the approximation power of convolution-based least squares versus interpolation," *IEEE Trans. Signal Processing*, vol. 45, pp. 1697–1711, July 1997.
- [24] W. H. Press, S. A. Teukolsky, W. T. Vetterling, and B. P. Flannery, *Numerical Recipes*. Cambridge, U.K.: Cambridge Univ. Press, 1992.
- [25] E. Cavanagh and B. D. Cook, "Numerical evaluation of Hankel transforms via Gaussian–Laguerre polynomial expansions," *IEEE Trans. Acoust., Speech, Signal Processing*, vol. ASSP-27, pp. 361–366, Aug. 1979.
- [26] A. Erdélyi, W. Magnus, F. Oberhettinger, and F. G. Tricomi, *Higher Transcendental Functions*. New York: McGraw-Hill, 1953, vol. II.



**Luc Knockaert** (M'88) received the Physical Engineer, Telecommunications Engineer, and Ph.D. degrees in electrical engineering from the University of Gent, Gent, Belgium, in 1974, 1977, and 1987, respectively.

From 1979 to 1984 and from 1988 to 1995, he was working on North–South cooperation and development projects at the Universities of Zaire and Burundi. He is currently a Senior Researcher at INTEC-IMEC, Gent. His current interests are the application of statistical and linear algebra methods in signal identification, Shannon theory, matrix compression, reduced-order modeling, and the use of integral transforms in electromagnetic problem solving. As author or co-author, he has contributed to about 25 international journal papers. Dr. Knockaert is a member of the ACM.